THE JOURNAL OF BIOLOGICAL CHEMISTRY VOL. 283, NO. 45, pp. 30942–30949, November 7, 2008

A Phosphate-binding Histidine of Binuclear Metallophosphodiesterase Enzymes Is a Determinant of 2′,3′-Cyclic Nucleotide Phosphodiesterase Activity*

Received for publication, July 2, 2008, and in revised form, August 18, 2008 Published, JBC Papers in Press, August 28, 2008, DOI 10.1074/jbc.M805064200

Niroshika Keppetipola and Stewart Shuman[1]

From the Molecular Biology Program, Sloan-Kettering Institute, New York, New York 10065

Binuclear metallophosphoesterases are an enzyme superfamily defined by a shared fold and a conserved active site. Although many family members have been characterized biochemically or structurally, the physiological substrates are rarely known, and the features that determine monoesterase *versus* diesterase activity are obscure. In the case of the dual phosphomonoesterase/diesterase enzyme *Cth*Pnkp, a phosphate-binding histidine was implicated as a determinant of 2′,3′-cyclic nucleotide phosphodiesterase activity. Here we tested this model by comparing the catalytic repertoires of *Mycobacterium tuberculosis* Rv0805, which has this histidine in its active site (His^{98}), and *Escherichia coli* YfcE, which has a cysteine at the equivalent position (Cys^{74}). We find that Rv0805 has a previously unappreciated 2′,3′-cyclic nucleotide phosphodiesterase function. Indeed, Rv0805 was 150-fold more active in hydrolyzing 2′,3′-cAMP than 3′,5′-cAMP. Changing His^{98} to alanine or asparagine suppressed the 2′,3′-cAMP phosphodiesterase activity of Rv0805 without adversely affecting hydrolysis of bis-*p*-nitrophenyl phosphate. Further evidence for a defining role of the histidine derives from our ability to convert the inactive YfcE protein to a vigorous and specific 2′,3′-cNMP phosphodiesterase by introducing histidine in lieu of Cys^{74}. YfcE-C74H cleaved the P–O2′ bond of 2′,3′-cAMP to yield 3′-AMP as the sole product. Rv0805, on the other hand, hydrolyzed either P–O2′ or P–O3′ to yield a mixture of 3′-AMP and 2′-AMP products, with a bias toward 3′-AMP. These reaction outcomes contrast with that of *Cth*Pnkp, which cleaves the P–O3′ bond of 2′,3′-cAMP to generate 2′-AMP exclusively. It appears that enzymic features other than the phosphate-binding histidine can influence the orientation of the cyclic nucleotide and thereby dictate the choice of the leaving group.

The binuclear metallophosphoesterases comprise a vast enzyme superfamily distributed widely among taxa. A prototypal member is bacteriophage λ phosphatase (λ-Pase),[2] which has been characterized structurally and biochemically (1–7). λ-Pase uses Mn^{2+} to catalyze phosphoester hydrolysis with a variety of substrates, including phosphopeptides, phosphoproteins, nucleoside 2′,3′-cyclic phosphates, and "generic" organic phosphomonoesters and diesters such as *p*-nitrophenyl phosphate and bis-*p*-nitrophenyl phosphate. Although the physiological substrate(s) and biological function of λ-Pase remain obscure, other well studied members of the binuclear metallophosphoesterase superfamily play key physiological roles in cellular pathways of signal transduction (*e.g.* the phosphoprotein phosphatase calcineurin), DNA repair (*e.g.* the DNA nuclease Mre11), or RNA processing (*e.g.* the RNA debranching enzyme Dbr1) (8–10).

The signature feature of the metallophosphoesterase superfamily is an active site composed of two metal ions (typically manganese, iron or zinc) coordinated with octahedral geometry by a cage of histidine, aspartate, and asparagine side chains (Fig. 1). The metals directly coordinate the scissile phosphate anion, as does the metal-binding asparagine. Plausible catalytic mechanisms have been proposed based on crystal structures of superfamily members with phosphate or sulfate in the active site (5, 9, 11–13) and mutational studies of a few exemplary enzymes. We construe the active site configuration of the *Mycobacterium tuberculosis* Rv0805 protein bound to a phosphate anion (14) to mimic the substrate complex of the phosphoesterase reaction (Fig. 1, *top panel*). In this structure, a metal-bridging water is situated 3 Å from the phosphorus atom. The almost perfectly apical orientation of this water to the putative "leaving" oxygen atom implicates the metal-bridged water as the nucleophile in the hydrolysis reaction. A putative mimetic of the product complex is exemplified by the active site of the *Escherichia coli* YfcE protein (15) (Fig. 1, *middle panel*). Here, the tetrahedral sulfate anion has undergone stereochemical inversion relative to the phosphate in Rv0805, and the former metal-bridged water is incorporated into the anion product.

The rapid pace of identification and structural/biochemical characterization of new members of the binuclear metallophosphoesterase superfamily via genome mining has not been matched by progress in understanding the biological functions and relevant substrates of most of these enzymes. The empirical approach is to produce recombinant protein and survey for activity with a broad a range of phosphoester substrates and then surmise a role based on the results. In this way, it was inferred that the *M. tuberculosis* Rv0805 enzyme depicted in Fig. 1 functions as a 3′,5′-cyclic nucleotide phosphodiesterase (16). By contrast, the *E. coli* YfcE protein catalyzed manganese-dependent hydrolysis of bis-*p*-nitrophenyl phosphate (15) but

* This work was supported, in whole or in part, by National Institutes of Health Grant GM42498. The costs of publication of this article were defrayed in part by the payment of page charges. This article must therefore be hereby marked "*advertisement*" in accordance with 18 U.S.C. Section 1734 solely to indicate this fact.

[1] American Cancer Society Research Professor. To whom correspondence should be addressed. E-mail: s-shuman@ski.mskcc.org.

[2] The abbreviations used are: λ-Pase, λ phosphatase; CIP, calf intestine phosphatase.

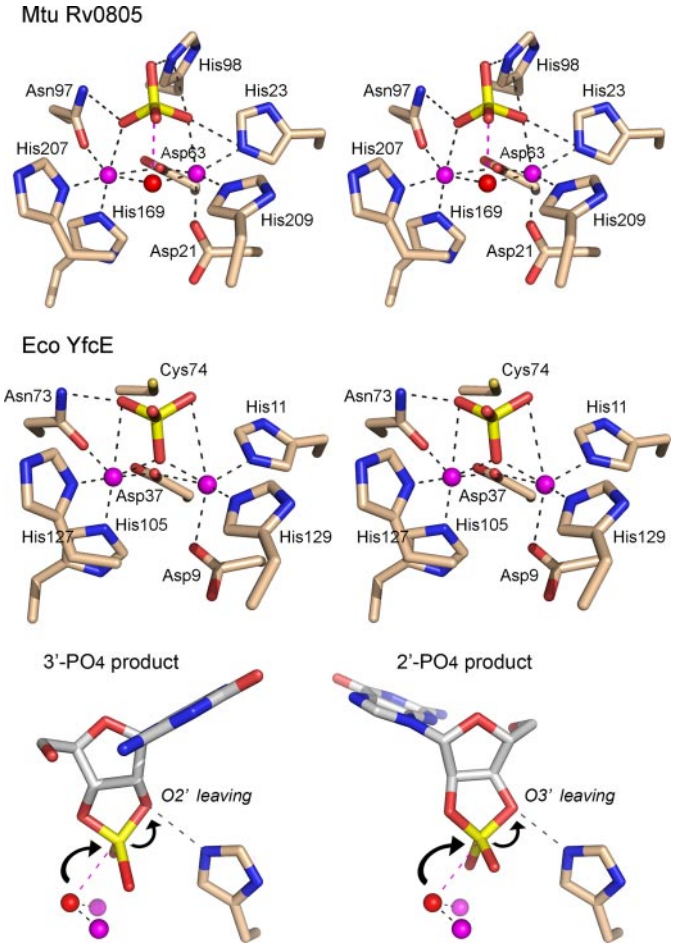

FIGURE 1. **Active sites of binuclear metallophosphodiesterases Rv0805 and YfcE.** The *top* and *middle panels* show stereo views of the active sites of *M. tuberculosis* Rv0805 (*top panel*; Protein Data Bank code 2HY1) and *E. coli* YfcE (*middle panel*; Protein Data Bank code 1SU1, protomer D). The amino acid side chains coordinating the binuclear metal cluster and either the phosphate ion in Rv0805 or sulfate ion in YfcE are shown. The metal ions are colored *magenta*. Water is colored *red*. The phosphate-binding histidine in Rv0805 (His^{98}) is replaced by a cysteine in YfcE (Cys^{74}). The *bottom panel* shows models of two potential orientations of 2′,3′-cGMP in the active site of Rv0805. The 2′,3′-cGMP molecule was imported from Protein Data Bank code 1GSP. The cyclic phosphate was superimposed on the phosphate anion in the Rv0805 structure. When the ribose O2′ is apical to the metal-bridged water nucleophile (*left*), the reaction yields a 3′-PO_4 nucleotide product. When the ribose O3′ atom is apical to the water nucleophile (*right*), the product is a 2′-PO_4 nucleotide. The His^{98} side chain is poised to donate a hydrogen bond to the leaving ribose oxygen atom in the modeled 2′,3′-cGMP substrate in either orientation.

had no activity with any natural phosphodiesters tested (nucleic acid, cyclic nucleotides, and phosphatidyl choline) or any of 57 natural phosphomonoester substrates (nucleotides, sugars, and amino acids).

Our studies have focused on *Clostridium thermocellum* polynucleotide kinase-phosphatase (*Cth*Pnkp) as a model to probe the binuclear metallophosphoesterase mechanism and the determinants of substrate specificity (7, 17–20). *Cth*Pnkp catalyzes 5′ and 3′ RNA end-healing reactions that prepare broken RNA termini for sealing by RNA ligase (17, 20). The central 3′ end-healing domain of *Cth*Pnkp belongs to the binuclear metallophosphoesterase superfamily; extensive mutational analysis underscores the strong similarity of the active site of *Cth*Pnkp to that of λ-Pase with respect to the metal and phosphate ligands (7, 18, 19). Biochemically, *Cth*Pnkp is a Ni^{2+}/Mn^{2+}-dependent phosphodiesterase/monoesterase, active on nucleotides (2′,3′-cAMP, 3′-AMP and 2′-AMP) and generic substrates (bis-*p*-nitrophenyl phosphate, *p*-nitrophenyl phosphate, and *p*-nitrophenyl phenylphosphonate). The phosphodiesterase and monoesterase reactions rely on overlapping but different ensembles of active site functional groups. The enzyme is remarkably plastic, insofar as *Cth*Pnkp can be transformed toward narrower metal and substrate specificities via mutations of the active site. For example, certain changes (*e.g.* replacing the metal-binding His^{189} residue with aspartate) transform *Cth*Pnkp into a Mn^{2+}-dependent phosphodiesterase devoid of monoesterase activity (19).

We have analyzed in depth the 2′,3′-cyclic phosphodiesterase activity of *Cth*Pnkp, in light of the fact that 2′,3′-cyclic phosphate termini are the predominant products of several known RNA damage pathways (7). We found that alanine, glutamine, or asparagine mutations at the phosphate-binding residue His^{264} of *Cth*Pnkp (corresponding to His^{76} in λ-Pase or His^{98} in Rv0805; Fig. 1) crippled the 2′,3′-cyclic phosphodiesterase activity, whereas the same changes enhanced the generic phosphodiesterase activity of *Cth*Pnkp with bis-*p*-nitrophenyl phosphate.

Our results prompted speculation that binuclear metallophosphoesterases might evolve distinct biochemical specificities via subtle changes at the active site (7). In particular, we predicted a correlation between 2′,3′-cyclic nucleotide phosphodiesterase activity and the presence of a phosphate-binding histidine analogous to His^{264}. In the present study, we tested this idea by comparing the repertoire of *M. tuberculosis* Rv0805, which has this histidine in its active site (His^{98}), with that of *E. coli* YfcE, which has a cysteine at the equivalent position (Cys^{74}). We find that Rv0805 has a vigorous 2′,3′-cyclic phosphodiesterase function (a property missed in earlier studies of this enzyme), and we characterize the activity here, especially its dependence on His^{98}. By introducing a histidine at the YfcE active site in lieu of Cys^{74}, we transform an inactive protein into a 2′,3′-cyclic phosphodiesterase.

EXPERIMENTAL PROCEDURES

Materials

p-Nitrophenyl phosphate, bis-*p*-nitrophenyl phosphate, *p*-nitrophenol, cAMP, cGMP, and cUMP were purchased from Sigma. Malachite green reagent was purchased from BIOMOL Research Laboratories.

Purification of Rv0805

The *M. tuberculosis* gene Rv0805 was amplified by two-stage overlap extension PCR (21) from genomic DNA with *Pfu* DNA polymerase using primers designed to eliminate an internal BamHI site while introducing an NdeI restriction site at the start codon and a BamHI site 3′ of the stop codon. The PCR product was digested with NdeI and BamHI and inserted into pET16b to generate an expression plasmid encoding the 318-amino acid Rv0805 polypeptide fused to an N-terminal His_{10} tag. Missense mutations H98N and H98A were introduced into the Rv0805 open reading frame by PCR using the two-stage overlap extension method (21). The inserts were sequenced to

verify that there were no unwanted coding changes. Wild type and mutant pET-Rv0805 plasmids were transformed into *E. coli* strain BL21(DE3). Cultures (200 ml) of *E. coli* BL21(DE3)/pET-Rv0805 were grown at 37 °C in Luria-Bertani medium containing 0.1 mg/ml ampicillin until the A_{600} reached ~0.6. The cultures were chilled on ice for 30 min, adjusted to 0.4 mM isopropyl-β-D-thiogalactopyranoside and 2% (v/v) ethanol, and then incubated at 17 °C for 16 h with continuous shaking. The cells were harvested by centrifugation, and the pellet was stored at −80 °C. All of the subsequent procedures were performed at 4 °C. Thawed bacteria were resuspended in 20 ml of buffer A (50 mM Tris-HCl, pH 7.5, 0.5 M NaCl, 10% sucrose). Lysozyme, phenylmethylsulfonyl fluoride, and Triton X-100 were added to final concentrations of 1 mg/ml, 1 mM, and 0.1%, respectively. The lysates were sonicated to reduce viscosity, and insoluble material was removed by centrifugation. The soluble extracts were applied to 1-ml columns of nickel-nitrilotriacetic acid-agarose (Qiagen) that had been equilibrated with buffer A. The columns were washed with 8 ml of the same buffer and then eluted stepwise with 4-ml aliquots of 25, 50, 200, and 500 mM imidazole in buffer B (50 mM Tris-HCl, pH 8.0, 0.5 M NaCl, 10% glycerol). The polypeptide compositions of the column fractions were monitored by SDS-PAGE. The His_{10}-Rv0805 proteins adsorbed to the column and were recovered predominantly in the 200 mM imidazole eluates. Protein concentrations were determined by using the Bio-Rad dye reagent with bovine serum albumin as the standard. The Rv0805 preparations were stored at −80 °C.

Purification of YfcE

The open reading frame encoding the 184-amino acid YfcE polypeptide was amplified from *E. coli* genomic DNA with primers that introduced an NdeI site at the start codon and a BamHI site 3′ of the stop codon. The PCR product was digested with NdeI and BamHI and inserted into pET16b to generate an expression plasmid encoding His_{10}-tagged YfcE. Missense mutations C74A, C74N, and C74H were introduced by PCR using the two-stage overlap extension method (21). The pET-YfcE plasmids were transformed into *E. coli* BL21(DE3). The His_{10}-YfceE proteins were purified from soluble extracts of 200-ml cultures of isopropyl-β-D-thiogalactopyranoside-induced bacteria as described above for His_{10}-Rv0805.

Hydrolysis of p-Nitrophenyl Phosphate and Bis-p-nitrophenyl Phosphate

Reaction mixtures (25 μl) containing 50 mM Tris-HCl (pH 8.5), 0.5 mM $MnCl_2$, 10 mM *p*-nitrophenyl phosphate or bis-*p*-nitrophenyl phosphate, and Rv0805 or YfcE as specified were incubated at 37 °C. The reactions were quenched by adding either 20 mM EDTA (YfcE reactions) or 5% SDS (Rv0805 reactions), followed by 0.9 ml of 1 M Na_2CO_3. Release of *p*-nitrophenol was determined by measuring A_{410} and interpolating the value to a *p*-nitrophenol standard curve.

Hydrolysis of Cyclic Nucleotides

Reaction mixtures (10 μl) containing 50 mM Tris-HCl (pH 8.5), 0.5 mM $MnCl_2$, 10 mM cyclic nucleotide as specified, and either Rv0805, YfcE, or calf intestine phosphatase (CIP) as specified were incubated for 10 min at 37 °C. (CIP was present in excess and did not limit the extent of phosphate release.) The reactions were quenched by adding 20 mM EDTA, followed by 1 ml of malachite green reagent. Release of phosphate was determined by measuring A_{620} and interpolating the value to a phosphate standard curve.

Kinetic Parameters

Hydrolysis of Bis-p-nitrophenyl Phosphate—Reaction mixtures (25 μl) containing 50 mM Tris-HCl (pH 8.5), 0.5 mM $MnCl_2$, increasing concentrations (0.313, 0.625, 1.25, 2.5, or 5.0 mM) of bis-*p*-nitrophenyl phosphate, and a fixed amount of the specified enzyme (2 pmol Rv0805 or YfcE-C74H corresponding to 0.08 μM enzyme; 5 pmol YfcE, 0.2 μM enzyme) were incubated at 37 °C for either 5 min (Rv0805 and YfcE-C74H) or 6 min (YfcE).

Hydrolysis of p-Nitrophenyl Phosphate—Reaction mixtures (25 μl) containing 50 mM Tris-HCl (pH 8.5), 0.5 mM $MnCl_2$, increasing concentrations (0.625, 1.25, 2.5, 5.0, or 10 mM) of *p*-nitrophenyl phosphate, and a fixed amount of the specified enzyme (100 pmol Rv0805 or YfcE, corresponding to 4 μM enzyme; 50 pmol YfcE-C74H, 2 μM enzyme) were incubated for 5 min at 37 °C.

Hydrolysis of 2′,3′-cAMP—Reaction mixtures (10 μl) containing 50 mM Tris-HCl (pH 8.5), 0.5 mM $MnCl_2$, 1 unit CIP, increasing concentrations (0.625, 1.25, 2.5, 5.0, or 10 mM) of 2′,3′-cAMP, and either 7.5 pmol Rv0805 (0.75 μM enzyme) or 25 pmol YfcE-C74H (2.5 μM enzyme) were incubated at 37 °C for 15 min (YfcE-C74H) or 5 min (Rv0805). The enzyme concentrations and incubation times were chosen to ensure that ≤36% of the substrate was converted to product at the lowest substrate concentrations tested (the ranges were from 9 to 36% conversion). The extents of *p*-nitrophenol or P_i production were first plotted as a function of substrate concentration. K_m and k_{cat} were then calculated from Eadie-Hofstee plots of the data. The K_m and k_{cat} values reported in Table 1 are averages from two independent substrate titration experiments ± mean absolute error.

RESULTS

2′,3′-Cyclic Phosphodiesterase Activity of M. tuberculosis Rv0805—Shenoy *et al.* (16) found that Rv0805 catalyzes Mn^{2+}-dependent cleavage of bis-*p*-nitrophenyl phosphate and hydrolysis of 3′,5′-cAMP to 5′-AMP. The ability of Rv0805 to hydrolyze 2′,3′-cyclic nucleotides was not reported. Here, we produced Rv0805 in *E. coli* as a His_{10} fusion and purified the enzyme from a soluble bacterial extract by nickel-agarose chromatography (Fig. 2). The recombinant protein hydrolyzed 10 mM bis-*p*-nitrophenyl phosphate in the presence of 0.5 mM $MnCl_2$ to yield *p*-nitrophenol; the extent of product formation was proportional to input enzyme (Fig. 3*A*). From the slope of the titration curve, we calculated a turnover number of 12.6 s^{-1}. Formation of *p*-nitrophenol by Rv0805 displayed a hyperbolic dependence on the concentration of bis-*p*-nitrophenyl phosphate (not shown). From an Eadie-Hofstee plot, we calculated a K_m of 0.9 mM and k_{cat} of 12.4 s^{-1} (Table 1). (The kinetic parameters reported previously by Shenoy *et al.* (16) were: K_m = 1.3 mM bis-*p*-nitrophenyl phosphate and k_{cat} = 4.2 s^{-1}.) Rv0805

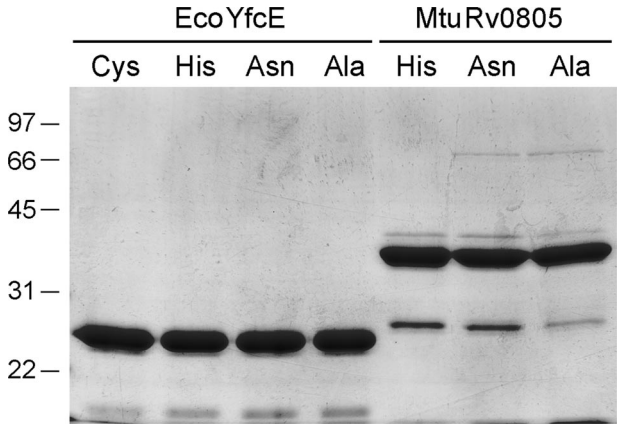

FIGURE 2. **Purification of Rv0805 and YfcE.** Aliquots (5 μg) of the nickel-agarose preparations of Rv0805 and YfcE containing the indicated amino acids at positions 98 and 74, respectively, were analyzed by SDS-PAGE. The Coomassie Blue-stained gel is shown. The mobility and sizes (kDa) of marker polypeptides are indicated on the *left*.

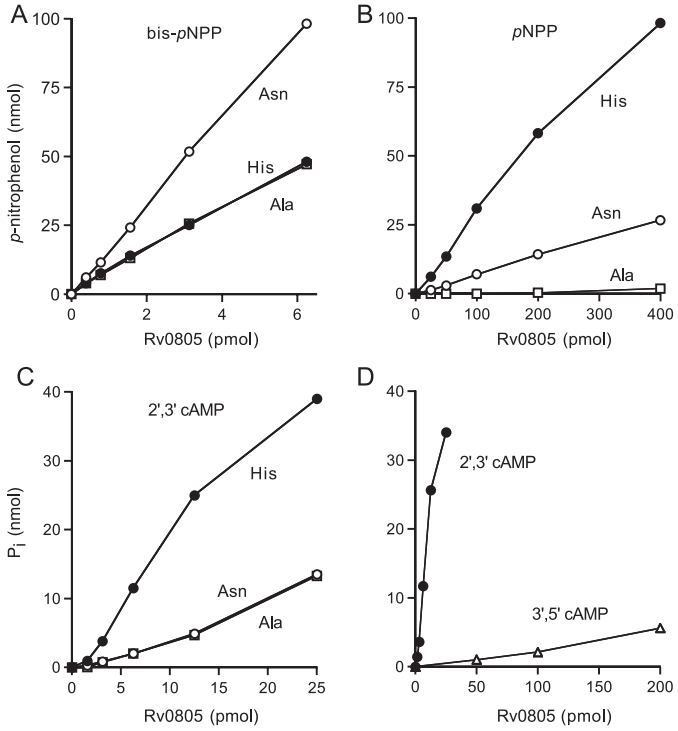

FIGURE 3. **Phosphoesterase activities of recombinant Rv0805 proteins.** *A*, hydrolysis of bis-*p*-nitrophenyl phosphate. Reaction mixtures (25 μl) containing 50 mM Tris-HCl (pH 8.5), 0.5 mM $MnCl_2$, 10 mM bis-*p*-nitrophenyl phosphate, and either wild type Rv0805, H98N, or H98A as specified (0.016, 0.031, 0.063, 0.125, or 0.25 μM enzyme) were incubated for 10 min at 37 °C. *B*, hydrolysis of *p*-nitrophenyl phosphate. Reaction mixtures (25 μl) containing 50 mM Tris-HCl (pH 8.5), 0.5 mM $MnCl_2$, 10 mM *p*-nitrophenyl phosphate, and either wild type Rv0805, H98N, or H98A as specified (1, 2, 4, 8, or 16 μM enzyme) were incubated for 10 min at 37 °C. *C*, hydrolysis of 2′,3′-cAMP. Reaction mixtures (10 μl) containing 50 mM Tris-HCl (pH 8.5), 0.5 mM $MnCl_2$, 10 mM 2′,3′-cAMP and either wild type Rv0805, H98N, or H98A as specified (0.16, 0.31, 0.62, 1.25, or 2.5 μM enzyme) were incubated for 10 min at 37 °C. *D*, reaction mixtures (10 μl) containing 50 mM Tris-HCl (pH 8.5), 0.5 mM $MnCl_2$, 10 mM of either 2′,3′-cAMP or 3′,5′-cAMP, 1 unit CIP, and wild type Rv0805 as specified (0.16, 0.31, 0.62, 1.25, or 2.5 μM enzyme for reactions containing 2′,3′-cAMP; 5, 10, or 20 μM enzyme for reactions containing 3′,5′-cAMP) were incubated for 10 min at 37 °C. The extents (nmol) of formation of *p*-nitrophenol (*A* and *B*) or inorganic phosphate (*C* and *D*) are plotted as a function of input enzyme (pmol). Each datum is the average of two separate experiments; mean absolute error bars are included for all points but may not be visible where the error is small.

displayed much weaker activity as a phosphomonoesterase (Fig. 3*B*). It hydrolyzed 10 mM *p*-nitrophenyl phosphate to *p*-nitrophenol with a specific activity of 0.5 s^{-1}. From the results of a substrate titration experiment, we calculated a K_m of 1.7 mM *p*-nitrophenyl phosphate and k_{cat} of 0.55 s^{-1} (Table 1). Thus, the catalytic efficiency (k_{cat}/K_m) of Rv0805 was 43-fold greater for the phosphodiesterase substrate.

2′,3′-Cyclic nucleotide phosphodiesterase activity was tested by reacting Rv0805 with 10 mM 2′,3′-cAMP in the presence of 0.5 mM $MnCl_2$. CIP was included in the reaction to liberate inorganic phosphate from any nucleoside phosphomonoesters formed by Rv0805. In the experiment shown in Fig. 4, Rv0805 converted 16% of the input 10 mM 2′,3′-cAMP to a CIP-sensitive phosphomonoester. By contrast, a control reaction with CIP alone released <1% of the P_i from 2′,3′-cAMP. Also, no free phosphate was released from 2′,3′-cAMP by Rv0805 in the absence of CIP.

To query whether Rv0805 displays specificity toward a particular nucleotide and whether the enzyme discriminates between a 2′,3′-cyclic phosphate and a 3′,5′-cyclic phosphate, we reacted the enzyme with 10 mM 2′,3′-cGMP, 3′,5′-cAMP, 3′,5′-cGMP, or 3′,5′-cUMP substrates. Rv0805 converted 16% of the input 2′,3′-cGMP to a CIP-sensitive phosphomonoester; thus, the enzyme did not have a preference for 2′,3′-cAMP *versus* 2′,3′-cGMP. The salient finding was that Rv0805 displayed much weaker activity as a 3′,5′-cyclic phosphodiesterase, converting only 0.2, 1, and 1.6% of the input 3′,5′-cAMP, 3′,5′-cGMP, and 3′,5′-cUMP substrates to CIP-sensitive phosphomonoesters, respectively (Fig. 4*A*). An enzyme titration experiment (Fig. 3*D*) showed that the specific activity of Rv0805 as a 2′,3′-cyclic AMP phosphodiesterase was 150-fold higher than as a 3′,5′-cyclic AMP phosphodiesterase (estimated turnover numbers of 150 and 1 min^{-1}, respectively). The kinetic data reported by Shenoy *et al.* (16) for hydrolysis of 3′,5′-cAMP indicated a k_{cat} value of ~1.7 min^{-1}, which agrees with the value we observe. Thus, the conclusion by Shenoy *et al.*, that Rv0805 is a 3′,5′-cyclic nucleotide phosphodiesterase, is open to question in light of our determination that it has 2 orders of magnitude higher activity with 2′,3′-cyclic nucleotide substrates. Additional experiments revealed that Rv0805 had essentially no detectable ability to hydrolyze phosphomonoester substrates 5′-AMP, 3′-AMP, or 2′-AMP (10 mM) in Tris-HCl buffer (pH 8.5) the presence of 0.5 mM $MnCl_2$. Specifically, a 10-μl reaction mixture so constituted with 21 μM Rv0805 released ≤0.1 nmol of inorganic phosphate (the lower limit of detection of the assay) as product from 100 nmol of input 5′-AMP, 3′-AMP, or 2′-AMP substrate during a 10-min incubation at 37 °C, which corresponds to a turnover number of ≤0.05 min^{-1}, a value 3,000-fold lower than the activity of Rv0805 with 2′,3′-cAMP.

Formation of a CIP-sensitive adenylate by Rv0805 displayed a hyperbolic dependence on the concentration of 2′,3′-cAMP. From an Eadie-Hofstee plot, we calculated a K_m of 1.6 mM and k_{cat} of 2.8 s^{-1} (Table 1). To determine the chemical identity of the products of the reaction with 2′,3′-cAMP, we performed cellulose TLC analysis of the reaction mixture as a function of enzyme in the presence of Rv0805 only (no CIP). The TLC plate was developed with buffer containing saturated ammonium

TABLE 1
Kinetic parameters for hydrolysis of bis-*p*-nitrophenyl phosphate (bis-*p*-NPP), *p*-nitrophenyl phosphate (*p*-NPP), and 2′,3′ cAMP

Enzyme	bis-*p*-NPP		*p*-NPP		2′,3′ cAMP	
	K_m	k_{cat}	K_m	k_{cat}	K_m	k_{cat}
	mM	s^{-1}	mM	s^{-1}	mM	s^{-1}
Rv0805	0.9 ± 0.12	12.4 ± 0.05	1.7 ± 0.1	0.55 ± 0.05	1.6 ± 0.4	2.8 ± 0.34
YfcE	4.8 ± 1.1	18 ± 2.6	10.6 ± 0.8	0.9 ± 0.1		
YfcE C74H	9.3 ± 1.6	72 ± 8	6.0 ± 0.9	3.0 ± 0.7	35 ± 7	2.95 ± 0.5

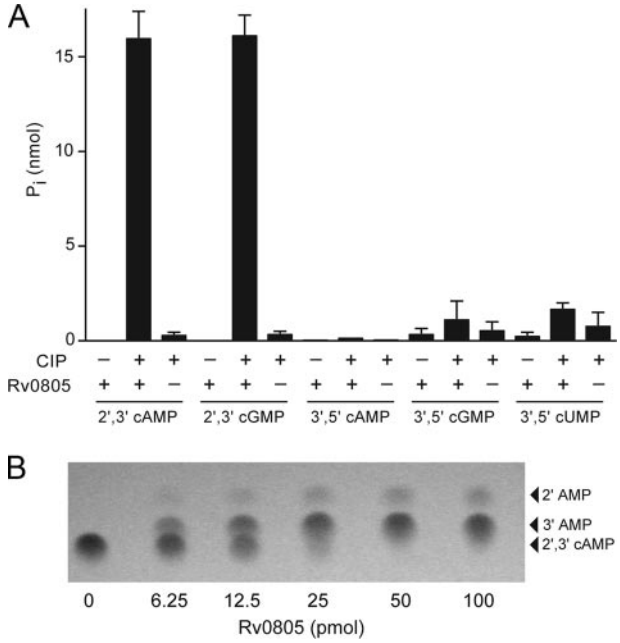

FIGURE 4. **Hydrolysis of cyclic phosphodiester substrates by Rv0805.** *A*, reaction mixtures (10 μl) containing 50 mM Tris-HCl (pH 8.0), 0.5 mM $MnCl_2$, 10 mM cNMP as specified, and Rv0805 (6.25 pmol; 0.625 μM) or CIP (1 unit) where indicated by + were incubated for 15 min at 37 °C. Each datum for P_i formation is the average of two separate experiments; mean absolute error bars are shown. *B*, product analysis. Reaction mixtures (10 μl) containing 50 mM Tris-HCl (pH 8.5), 0.5 mM $MnCl_2$, 10 mM 2′,3′-cAMP, and wild type Rv0805 as specified (corresponding to 0, 0.62, 1.25, 2.5, 5.0, or 10 μM enzyme) were incubated for 5 min at 37 °C. The reactions were quenched with EDTA. Aliquots (1 μl) of each sample were applied to a cellulose-F TLC plate (EMD chemicals). Ascending TLC was performed with buffer containing saturated ammonium sulfate, 3 M sodium acetate, isopropanol (80/6/2). The nucleotides were visualized by photography under UV light. The positions of the 2′,3′-cAMP, 3′-AMP and 2′-AMP standards are indicated on the *right*.

sulfate, 3 M sodium acetate, isopropanol (80/6/2), in which the order of migration away from the origin (R_f) is 2′,3′-cAMP < 3′-AMP < 2′-AMP (22). This experiment revealed a quantitative conversion of 2′,3′ cAMP to a mixture of more quickly moving products. The major species corresponded to 3′-AMP, and the minor product migrated as 2′-AMP (Fig. 4*B*). Their proportions did not change over the range of Rv0805 concentrations tested, arguing against a precursor-product relationship between the major and minor species. Thus, we conclude that Rv0805 preferentially cleaves the P–O2′ bond of 2′,3′-cAMP.

Effect of His[98] Mutations on the 2′,3′-Cyclic Phosphodiesterase Activity of Rv0805—We produced and purified Rv0805 mutants with alanine or asparagine in place of His[98] (Fig. 2). The specific activity of the H98A protein in hydrolysis of bis-*p*-nitrophenyl phosphate was identical to that of wild type Rv0805, whereas the specific activity of H98N was 2-fold higher than the wild type value (Fig. 3*A*). By contrast, the H98A mutation virtually abolished phosphomonoesterase activity on the *p*-nitrophenyl phosphate substrate (Fig. 3*B*). The specific activity of the H98N protein with *p*-nitrophenyl phosphate (0.12 s^{-1}) was one-fourth the wild type level (Fig. 3*B*). The salient findings were that the H98A and H98N changes both suppressed the 2′,3′-cAMP phosphodiesterase specific activity to one-fifth the level of wild type Rv0805 (Fig. 3*C*). These selective inhibitory effects of His[98] mutations on hydrolysis of 2′,3′-cAMP (and *p*-nitrophenyl phosphate) but not bis-*p*-nitrophenyl phosphate are in accord with the mutational effects seen for His[264] in *Cth*Pnkp (7, 19).

Phosphodiesterase Activity of E. coli YfcE—Miller *et al.* (15) characterized *E. coli* YfcE protein as a Mn^{2+}-dependent phosphodiesterase that cleaved bis-*p*-nitrophenyl phosphate, thymidine 5′-monophosphate-*p*-nitrophenyl ester, and *p*-nitrophenyl phosphorylcholine but was unable to hydrolyze 2′,3′- or 3′,5′-cyclic nucleotide phosphodiesters or any of 57 different phosphomonoesters, including *p*-nitrophenyl phosphate. The crystal structure of YfcE with metals and sulfate in the active site (15) reveals that YfcE has a cysteine (Cys[74]) at the position equivalent to Rv0805 His[98] and *Cth*Pnkp His264 (Fig. 1). We seized on YfcE as a promising scaffold to test the key prediction of our substrate-specificity model, by engineering a gain-of-function in a metallophosphoesterase enzyme that ordinarily lacks the ability to hydrolyze 2′,3′-cyclic nucleotides.

We produced wild type YfcE as a His_{10} fusion and purified it from a soluble bacterial extract by nickel-agarose chromatography (Fig. 2). YfcE hydrolyzed 10 mM bis-*p*-nitrophenyl phosphate in the presence of 0.5 mM $MnCl_2$ to yield *p*-nitrophenol; from the slope of the titration curve (Fig. 5*A*), we estimated a turnover number of 22 s^{-1}. From the results of a substrate titration experiment, we calculated a K_m of 4.8 mM bis-*p*-nitrophenyl phosphate and a k_{cat} of 18 s^{-1} (Table 1). (The kinetic parameters reported previously by Miller *et al.* (15) were: K_m = 9.7 mM bis-*p*-nitrophenyl phosphate and k_{cat} of 20 s^{-1}.) Unlike Miller *et al.*, we were able to detect a generic YfcE phosphomonoesterase activity. YfcE hydrolyzed 10 mM *p*-nitrophenyl phosphate to *p*-nitrophenol in an enzyme concentration-dependent manner (Fig. 5*B*). From the slope of the titration curve, we estimated a turnover number of 0.4 s^{-1}. Kinetic parameters for the YfcE phosphomonoesterase reaction determined from a substrate titration experiment were: K_m = 10.6 mM *p*-nitrophenyl phosphate and k_{cat} = 0.9 s^{-1} (Table 1). The catalytic efficiency (k_{cat}/K_m) of YfcE is thereby 44-fold greater for the generic phosphodiesterase substrate. YfcE had feeble activity in hydrolysis of 2′,3′-cAMP to a CIP-sensitive nucleoside monoester (Fig. 5*C*). From the slope of the titration curve, we estimated a turnover number of 0.03 s^{-1}.

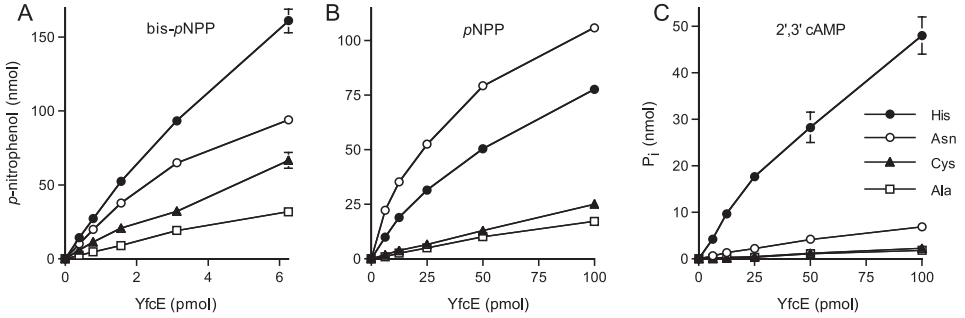

FIGURE 5. **Phosphoesterase activities of recombinant YfcE proteins.** *A*, hydrolysis of bis-*p*-nitrophenyl phosphate. Reaction mixtures (25 μl) containing 50 mM Tris-HCl (pH 8.5), 0.5 mM $MnCl_2$, 10 mM bis-*p*-nitrophenyl phosphate, and either wild type YfcE, C74H, C74N, or C74A as specified (0.016, 0.031, 0.062, 0.125, or 0.25 μM enzyme) were incubated for 10 min at 37 °C. *B*, hydrolysis of *p*-nitrophenyl phosphate. Reaction mixtures (25 μl) containing 50 mM Tris-HCl (pH 8.5), 0.5 mM $MnCl_2$, 10 mM *p*-nitrophenyl phosphate, and either wild type YfcE, C74H, C74N, or C74A as specified (0.25, 0.5, 1, 2, or 4 μM enzyme) were incubated for 10 min at 37 °C. *C*, hydrolysis of 2′,3′-cAMP. Reaction mixtures (10 μl) containing 50 mM Tris-HCl (pH 8.5), 0.5 mM $MnCl_2$, 10 mM 2′,3′-cAMP, and either wild type, C74H, C74N, or C74A as specified (0.625, 1.25, 2.5, 5, or 10 μM enzyme) were incubated for 15 min at 37 °C. The extents (nmol) of formation of *p*-nitrophenol (*A* and *B*) or inorganic phosphate (*C*) are plotted as a function of input enzyme (pmol). Each datum is the average of two separate experiments; mean absolute error bars are included for all points but may not be visible where the error is small.

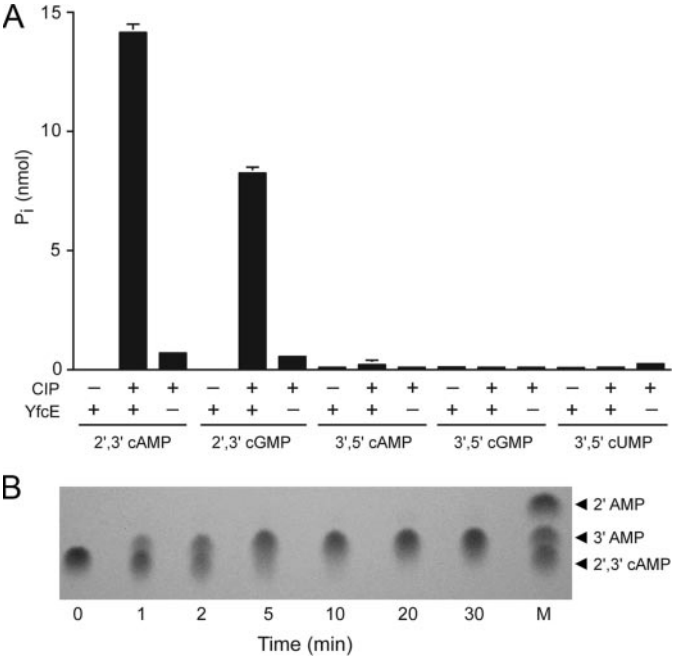

FIGURE 6. **Hydrolysis of cyclic phosphodiester substrates by YfcE-C74H.** *A*, reaction mixtures (10 μl) containing 50 mM Tris-HCl (pH 8.5), 0.5 mM $MnCl_2$, 10 mM substrate as specified, and YfcE-C74H (25 pmol; 2.5 μM enzyme) or CIP (1 unit) where indicated by + were incubated for 15 min at 37 °C. Each datum for P_i formation is the average of two separate experiments; mean absolute error bars are included for all data but may not be visible where the error is small. *B*, product analysis. A reaction mixture (90 μl) containing 50 mM Tris-HCl (pH 8.5), 0.5 mM $MnCl_2$, 10 mM 2′,3′-cAMP, and 45 μg of YfcE-C74H (13.5 μM enzyme) were incubated at 37 °C. Aliquots (10 μl) were withdrawn at the times specified and quenched immediately with EDTA. 1 μl of each sample was applied to a cellulose-F TLC plate. Markers 2′-AMP, 3′-AMP, and 2′,3′-cAMP (5 nmol each) were spotted in *lane M*. TLC was performed as described in Fig. 4. The nucleotides were visualized by photography under UV light.

Transformation of YfcE into a 2′,3′-Cyclic Nucleotide Phosphodiesterase—YfcE mutants with alanine, asparagine, or histidine in lieu of Cys^{74} were purified (Fig. 2) and surveyed for phosphodiesterase and monoesterase activities (Fig. 5). The specific activities in hydrolysis of bis-*p*-nitrophenyl phosphate (Fig. 5*A*) varied within a 5-fold range according to the amino acid at position 74, as follows: His (56 s^{-1}) > Asn (40 s^{-1}) > Cys (22 s^{-1}) > Ala (10 s^{-1}). Greater salutary effects of the histidine and asparagine changes were observed for phosphomonoesterase activity with *p*-nitrophenyl phosphate (Fig. 5*B*), with the following hierarchy of specific activities: Asn (6 s^{-1}) > His (2.5 s^{-1}) > Cys (0.4 s^{-1}) ≈ Ala (0.3 s^{-1}). The increase of generic Mn^{2+}-dependent monoesterase activity in YfcE-C74H *versus* C74A reciprocated the loss of generic monoesterase function observed when the Rv0805 and *Cth*Pnkp histidines were mutated to alanine. The YfcE-C74N and C74H titration curves deviated downward from linearity at the higher levels of input enzyme at which ≥30% of the 10 mM *p*-nitrophenyl phosphate substrate was converted to *p*-nitrophenol and P_i (Fig. 5*B*). This reflected product inhibition by P_i. From a separate experiment entailing prior addition of increasing amounts of phosphate to a reaction mixture containing 10 mM *p*-nitrophenyl phosphate and 0.2 μM YfcE-C74H, we determined an IC_{50} value of 2.5 mM P_i (data not shown).

The instructive finding was that the C74H mutation uniquely conferred a gain of function in hydrolysis of 10 mM 2′,3′-cAMP (Fig. 5*C*). From the slope of the titration curve, we estimated a turnover number of 1.3 s^{-1}. To delineate the specificity of this novel catalyst, we tested C74H cyclic phosphodiesterase activity in parallel with 10 mM 2′,3′-cAMP, 2′,3′-cGMP, 3′,5′-cAMP, 3′,5′-cGMP, and 3′,5′-cUMP substrates (Fig. 6*A*). This experiment highlighted YfcE-C74H as strictly specific for 2′,3′-cNMPs; there was scant activity with the 3′,5′-cNMP substrates. Control assays verified that YfcE-C74H catalyzed no detectable phosphate release from 2′,3′-cAMP in the absence of CIP (Fig. 6*A*). Moreover, YfcE-C74H had no detectable ability to hydrolyze phosphomonoester substrates 5′-AMP, 3′-AMP, or 2′-AMP (10 mM) in the presence of 0.5 mM $MnCl_2$ to yield inorganic phosphate as product. Specifically, a 10-μl reaction mixture so constituted with 140 μM YfcE-C74H released ≤0.1 nmol of inorganic phosphate (the lower limit of detection of the assay) as product from 100 nmol of input 5′-AMP, 3′-AMP, or 2′-AMP substrate during a 15-min incubation at 37 °C, which corresponds to a turnover number of ≤0.005 min^{-1}, a value 15,000-fold lower than the activity of YfcE-C74H with 2′,3′-cAMP.

To determine the chemical identities of the products of the reaction with 2′,3′-cAMP, we performed cellulose TLC analysis of the reaction mixture as a function of reaction time in the presence of YfcE-C74H only (no CIP). YfcE-C74H quantitatively converted the 2′,3′-cAMP substrate to a single product that comigrated with the 3′-AMP standard (Fig. 6*B*). We conclude that YfcE-C74H cleaves exclusively the P–O2′ bond of 2′,3′-cAMP. Steady-state kinetic parameters for the YfcE-C74H cyclic phosphodiesterase derived from 2′,3′-cAMP titra-

tion experiments were as follows: K_m = 35 mM 2′,3′-cAMP and k_{cat} = 2.95 s^{-1} (Table 1). It is notable that the k_{cat} of the "designed" YfcE-C74H 2′,3′-cAMP phosphodiesterase was similar to that of the "natural" Rv0805 enzyme, although the affinity of the YfcE-C74H protein for the substrate was 22-fold less than Rv0805.

These results attest to the transformative power of the active site histidine as a determinant of cyclic nucleotide phosphodiesterase activity. As discussed below, we surmise that enzymic groups other than the phosphate-binding histidine might contribute to cyclic nucleotide binding and orientation of the leaving group.

DISCUSSION

The present study supports a model, suggested by our studies of *Cth*Pnkp (7), that the presence of a phosphate-binding histidine in the active site of phosphodiesterase members of the binuclear metallophosphoesterase superfamily is a determinant of 2′,3′-cyclic nucleotide phosphodiesterase activity. Here we focused on two structurally characterized metallophosphoesterases that differ in having a histidine (Rv0805) or a cysteine (YfcE) at this active site position. Although Rv0805 had been dubbed a 3′,5′-cyclic nucleotide phosphodiesterase by other investigators (16), our characterization of this enzyme shows it to be 150-fold more active on 2′,3′-cAMP than 3′,5′-cAMP. Thus, the presence of an active site histidine in Rv0805 correctly predicted its heretofore unexamined capacity for 2′,3′-cNMP hydrolysis. Changing the histidine to alanine or asparagine suppressed 2′,3′-cAMP phosphodiesterase activity of Rv0805 without affecting the hydrolysis of a generic non-nucleotide phosphodiester substrate. Even more compelling evidence for the defining role of the histidine derives from our ability to convert the otherwise inactive YfcE protein into an active and highly specific 2′,3′-cNMP phosphodiesterase by introducing a histidine in lieu of Cys^{74}.

The correlation of an active site histidine and 2′,3′-cNMP phosphodiesterase activity applies to other metallophosphoesterase superfamily members, including λ-Pase (7) and the recently characterized *Deinococcus radiodurans* enzyme DR1281 (23). DR1281 resembles Rv0805 in its ~35-fold higher k_{cat} for Mn^{2+}-dependent hydrolysis of bis-*p*-nitrophenyl phosphate *versus p*-nitrophenyl phosphate and its selective hydrolysis of 2′,3′-cNMPs *versus* 3′,5′-cNMPs (23). The correlation between a nonhistidine residue and the absence of cyclic phosphodiesterase activity seen here with YfcE is reminiscent of the properties of the structurally characterized *Methanococcus jannaschii* enzyme MJ0936 (24). MJ0936 has vigorous activity in hydrolyzing bis-*p*-nitrophenyl phosphate but is unable to cleave *p*-nitrophenyl phosphate. Although possessed of a generic phosphodiesterase activity, MJ0936 reportedly had no detectable cyclic phosphodiesterase activity with the 2′,3′- or 3′,5′-forms of cAMP or cGMP (24). The crystal structure of manganese-bound MJ0936 (Protein Data Bank code 1S3N) (24) reveals the similarity of its active site to that of Rv0805, except for the presence of an asparagine in lieu of the phosphate-coordinating histidine.

Although the histidine is clearly a major determinant of 2′,3′-cNMP phosphodiesterase activity, the outcomes of the hydrolysis step can differ significantly from one enzyme to another. *Cth*Pnkp-H189D (a diesterase-only mutant in which a metal-binding histidine is changed to aspartate) catalyzes hydrolysis of the P–O3′ bond of 2′,3′-cAMP or -cGMP to yield exclusively 2′-AMP or 2′-GMP products (7, 20). By contrast, YfcE-C74H (Fig. 6) and DR1281 (23) both catalyze hydrolysis of the P–O2′ bond of 2′,3′-cAMP to yield 3′-AMP as the sole product. Rv0805, on the other hand, can hydrolyze either P–O2′ or P–O3′ to yield a mixture of 3′-AMP and 2′-AMP products, with a clear bias toward generation of 3′-AMP (Fig. 3). λ-Pase also hydrolyzes either P–O2′ or P–O3′ to yield both 3′-AMP and 2′-AMP products, albeit with a preference for 2′-AMP formation (7). We surmise that the histidine facilitates an aspect of phosphohydrolase chemistry common to both pathways (conceivably entailing proton donation to the ribose O2′ or O3′ leaving atom), but constituents other than the histidine dictate the reaction outcome by influencing substrate orientation and affinity.

The critical issue of substrate orientation in determining which products are formed is illustrated in Fig. 1 (*bottom panel*), in which we have modeled a 2′,3′-cGMP molecule (imported from a crystal structure of RNase T1; Protein Data Bank code 1GSP) (33) into the active site of Rv0805 by superimposing the cyclic phosphate moiety of cGMP on the phosphate anion in the Rv0805 structure. This results in two potential configurations for opening the cyclic phosphate. When the ribose O2′ is apical to the metal-bridged water nucleophile, the reaction yields a 3′-PO_4 nucleotide product. When the ribose O3′ atom is apical to the water nucleophile, the product is a 2′-PO_4 nucleotide. The His^{98} side chain is poised to donate a hydrogen bond to the leaving ribose oxygen atom in the modeled substrate complex with 2′,3′-cGMP in either orientation (Fig. 1, *bottom panel*). The asymmetry of the binding modes is apparent in the locations of the bulky purine base relative to the (pseudo-mirror-symmetrical) cyclic phosphate-ribose ring system. It is likely that steric constraints on the adoption of one orientation *versus* the other are responsible for stringent and opposite choice of leaving groups during the 2′,3′-cNMP phosphodiesterase reactions of *Cth*Pnkp-H189D *versus* YfcE-C74H and DR1281. We speculate that Rv0805 and λ-Pase are less constrained with respect to the binding orientations of the cyclic nucleotide, thereby allowing formation of either 2′-NMP or 3′-NMP products. Further evaluation of this hypothesis and elucidation of the structural elements that dictate substrate orientation, will hinge on determining crystal structures of metallophosphodiesterase enzymes with a 2′,3′-cyclic nucleotide bound in the active site.

Are there useful biological inferences to be drawn from the fact that a metallophosphodiesterase family member has a vigorous and relatively specific 2′,3′-cyclic nucleotide phosphodiesterase activity *in vitro*? In the case of *Cth*Pnkp, we have suggested that this activity is relevant to the repair of RNA 2′,3′-cyclic ends (7, 20), which are natural intermediates in RNA processing (25) and RNA catabolism (26). RNA 2′,3′-cyclic ends are also the end products of RNA-cleaving toxins (27–30). An initial clue to a nucleic acid repair role for *Cth*Pnkp was the covalent linkage of its metallophosphoesterase domain to a polynucleotide kinase module (17) that is known to catalyze 5′

end healing reactions in RNA repair pathways (25, 27). In the case of Rv0805 and λ-Pase, there are no physiologically instructive flanking domains, and there is, to our knowledge, no genetic evidence implicating either protein in a particular biological process in its native context. The prospect that *M. tuberculosis* Rv0805 acts on broken RNAs is worthy of consideration, given that *M. tuberculosis* encodes at least seven MazF-like endoribonuclease toxins that generate site-specific breaks with 2′,3′-cyclic ends (30–32).

Finally, the correlation between a nonhistidine residue (Cys^{74}) in the YfcE active site and the absence of cyclic phosphodiesterase activity hints at a novel specificity within the superfamily. We think it is unlikely that the histidine substitution by cysteine in YfcE is a sporadic event resulting in a "crippled" metallophosphodiesterase diesterase enzyme. Indeed, Miller *et al.* (15) described a novel clade of bacterial YfcE-like binuclear metallophosphoesterases, embracing predicted polypeptides from diverse bacterial genera, each of which has a cysteine in lieu of the phosphate-binding histidine. A current data base search identifies members of this cysteine-containing bacterial subfamily in *Shigella*, *Citrobacter*, *Enterobacter*, *Klebsiella*, *Yersinia*, *Serratia*, *Erwinia*, *Vibrio*, *Shewanella*, *Photobacterium*, *Aeromonas*, *Clostridium*, *Bacteroides*, *Ruminococcus*, *Thermotoga*, *Moorella*, *Treponema*, and others. The fact that YfcE can hydrolyze 2′,3′-cNMPs when mutated to His^{74} hints that this subfamily evolved toward a narrow substrate specificity. The "real" substrate for YfcE-like phosphodiesterases (and thus the specificity determining role of the active site cysteine) remains to be discovered.

REFERENCES

1. Cohen, P. T. W., and Cohen, P. (1989) *Biochem. J.* **260,** 931–934
2. Barik, S. (1993) *Proc. Natl. Acad. Sci. U. S. A.* **90,** 10633–10637
3. Zhuo, S., Clemens, J. C., Hakes, D. J., Barford, D., and Dixon, J. E. (1993) *J. Biol. Chem.* **268,** 17754–17761
4. Mertz, P., Yu, L., Sikkink, R., and Rusnak, F. (1997) *J. Biol. Chem.* **272,** 21296–21302
5. Voegtli, W. C., White, D. J., Reiter, N. J., Rusnak, F., and Rosenzweig, A. C. (2000) *Biochemistry* **39,** 15365–15374
6. White, D. J., Reiter, N. J., Sikkink, R. A., Yu, L., and Rusnak, F. (2001) *Biochemistry* **40,** 8918–8929
7. Keppetipola, N., and Shuman, S. (2007) *Nucleic Acids Res.* **35,** 7721–7732
8. Rusnak, F., and Mertz, P. (2000) *Physiol. Rev.* **80,** 1483–1521
9. Hopfner, K. P., Karcher, A., Craig, L., Woo, T. T., Carney, J. P., and Tainer, J. A. (2001) *Cell* **105,** 473–485
10. Khalid, F., Damha, M., Shuman, S., and Schwer, B. (2005) *Nucleic Acids Res.* **33,** 6349–6360
11. Klabunde, T., Sträter, N., Fröhlich, R., Witzel, H., and Krebs, B. (1996) *J. Mol. Biol.* **259,** 737–748
12. Knöfel T., and Sträter, N. (2001) *J. Mol. Biol.* **309,** 239–254
13. Schenk, G., Gahan, L. R., Carrington, L. E., Mitic, N., Valizadeh, M., Hamilton, S. E., de Jersey, J., and Guddat, L. W. (2005) *Proc. Natl. Acad. Sci. U. S. A.* **102,** 273–278
14. Shenoy, A. R., Capuder, M., Draskovic, P., Lamba, D., Visweswariah, S. S., and Podobnik, M. (2007) *J. Mol. Biol.* **365,** 211–225
15. Miller, D. J., Shuvalova, L., Evdokimova, E., Savchenko, A., Yakunin, A. F., and Anderson, W. F. (2007) *Protein Sci.* **16,** 1338–1348
16. Shenoy, A. R., Sreenath, N., Podobnik, M., Kovacevic, M., and Visweswariah, S. S. (2005) *Biochemistry* **44,** 15695–15704
17. Martins, A., and Shuman, S. (2005) *RNA* **11,** 1271–1280
18. Keppetipola, N., and Shuman, S. (2006) *RNA* **12,** 73–82
19. Keppetipola, N., and Shuman, S. (2006) *Biol. Chem.* **281,** 19251–19259
20. Keppetipola, N., Nandakumar, J., and Shuman, S. (2007) *Nucleic Acids Res.* **35,** 3624–3630
21. Ho, S. N., Hunt, H. D., Horton, R. M., Pullen, J. K., and Pease, L. R. (1989) *Gene* (*Amst.*) **77,** 51–59
22. Genshik, P., Billy, E., Swianiewicz, M., and Filipowicz, W. (1997) *EMBO J.* **16,** 2955–2967
23. Shin, D. H., Proudfoot, M., Lim, H. J., Choi, I. K., Yokota, H., Yakunin, A. F., Kim, R., and Kim, S. H. (2008) *Proteins* **70,** 1000–1009
24. Chen, S., Yakunin, A. F., Kuznetsova, E., Busso, D., Pufan, R., Proudfoot, M., Kim, R., Kim, S. H. (2004) *J. Biol. Chem.* **279,** 31854–31862
25. Abelson, J., Trotta, C. R., and Li, H. (1998) *J. Biol. Chem.* **273,** 12685–12688
26. Raines, R. T. (1998) *Chem. Rev.* **98,** 1045–1065
27. Amitsur, M., Levitz, R., and Kaufman, G. (1987) *EMBO J.* **6,** 2499–2503
28. Ogawa, T., Tomita, K., Ueda, T., Watanabe, K., Uozumi, T., and Masaki, H. (1999) *Science* **283,** 2097–2100
29. Tomita, K., Ogawa, T., Uozumi, T., Watanabe, K., and Masaki, H. (2000) *Proc. Natl. Acad. Sci. U. S. A.* **97,** 8278–8283
30. Zhang, Y., Zhang, J., Hara, H., Kato, I., and Inouye, M. (2005) *J. Biol. Chem.* **280,** 3143–3150
31. Zhu, L., Zhang, Y., Teh, J., Zhang, J., Connell, N., Rubin, H., and Inouye, M. (2006) *J. Biol. Chem.* **281,** 18638–18643
32. Zhu, L., Phadatare, S., Nariya, H., Ouyang, M., Husson, R. N., and Inouye, M. (2008) *Mol. Microbiol.* **69,** 559–569
33. Zegers, I., Loris, R., Dehollander, G., Haikal, A. F., Poortmans, F., Steyaert, J., and Wyns, L. (1998) *Nat. Struct. Biol.* **5,** 280–283